

ATLAS measurements of CP-violation and rare decay processes with beauty mesons

Lake Louise Winter Institute 2022
Alberta, Canada, 20 to 26 February 2022

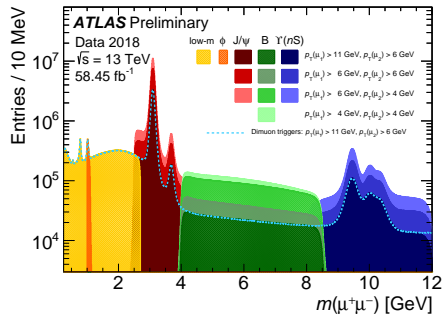
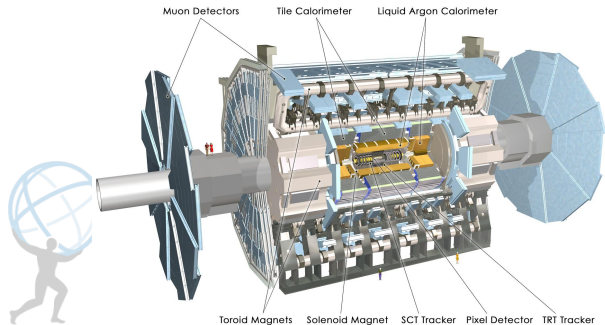
Tomáš Jakoubek on behalf of the ATLAS Collaboration

Weizmann Institute of Science
tomas.jakoubek@cern.ch

Introduction

B-physics at ATLAS

- ATLAS Run 2: 139 fb^{-1} of pp collisions at $\sqrt{s} = 13 \text{ TeV}$ collected in 2015-2018 (Run 1: 25 fb^{-1} at 7 and 8 TeV).
- Producing $2.5\text{M } b\bar{b}$ pairs/second, B_s , B_c , Λ_b , etc. available.
- Focus mostly on final states with muons, fully reconstructable.
- Typical trigger: low- p_T di-muons at low invariant mass, using information from tracker and muon detectors. Rate up to $\sim 200 \text{ Hz}$.
- In 2018, a di-electron high-level trigger (HLT) implemented and being analysed now.



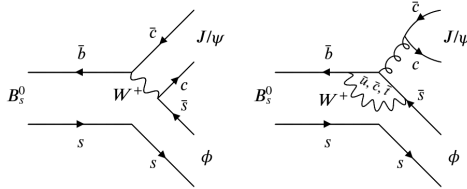
Measurement of the CP -violating phase ϕ_s in
 $B_s^0 \rightarrow J/\psi\phi$ decays in ATLAS at 13 TeV



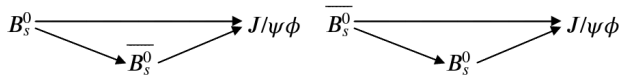
CPV in $B_s^0 \rightarrow J/\psi\phi$: Introduction

Eur. Phys. J. C 81 (2021) 342

- Decay $B_s^0 \rightarrow J/\psi\phi$ is expected to be sensitive to new physics (NP) contributions to CP -violation.



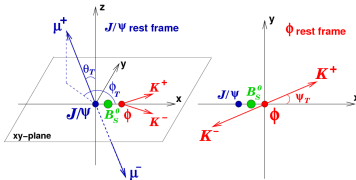
- Neutral B_s^0 meson can oscillate into its antiparticle \overline{B}_s^0 (and vice versa).
- The oscillation frequency is characterized by the mass difference Δm_s of the heavy (B_H) and light (B_L) mass eigenstates.
- In the absence of CP violation, the B_H state would correspond to the CP -odd state and the B_L to the CP -even state.
- CP violation in interference of mixing and decay:** the common final state is reached via two different decay chains:



CPV in $B_s^0 \rightarrow J/\psi\phi$: Measurement

Eur. Phys. J. C 81 (2021) 342

- CP-violating phase is defined as the weak phase difference between the $B_s^0 - \bar{B}_s^0$ mixing amplitude and the $b \rightarrow c\bar{c}s$ decay amplitude.
- In the Standard Model (SM) it can be related to the CKM matrix $\phi_s \simeq -2\beta_s = -2 \arg\left(-\frac{V_{cs}V_{cb}^*}{V_{cs}V_{cb}^*}\right)$ and then $\phi_s = -0.03696_{-0.00082}^{+0.00072}$ rad can be predicted [1].
- Any sizeable deviation from this value would be a sign of beyond SM physics.
- $B_s^0 \rightarrow J/\psi\phi$: pseudoscalar to vector-vector final state \rightarrow admixture of CP-odd ($L = 1$) and CP-even ($L = 0, 2$) states. Distinguishable through time-dependent angular analysis.
- Non-resonant S-wave decay $B_s^0 \rightarrow J/\psi K^+ K^-$ and $B_s^0 \rightarrow J/\psi f_0$ both contribute to the final state:
 - can't be identified in the measured data, but can significantly bias measurement of ϕ_s ,
 - thus they have to be included in the differential decay rate (due to interference with the signal decay) and treated by the fit.



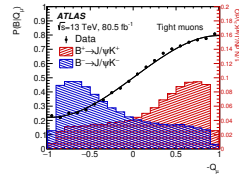
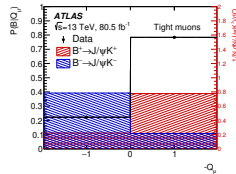
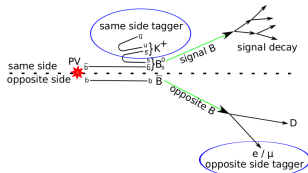
k	$\mathcal{O}^{(k)}(t)$	$g^{(k)}(\theta_T, \psi_T, \phi_T)$
1	$\frac{3}{2} A_0(0) ^2 \left[(1 + \cos \phi_s) e^{-\Gamma_1 t} + (1 - \cos \phi_s) e^{-\Gamma_2 t} \pm 2e^{-\Gamma t} \sin(\Delta m_s t) \sin \phi_s \right]$	$2 \cos^2 \psi_T (1 - \sin^2 \theta_T \cos^2 \phi_T)$
2	$\frac{3}{2} A_{ }(0) ^2 \left[(1 + \cos \phi_s) e^{-\Gamma_1 t} + (1 - \cos \phi_s) e^{-\Gamma_2 t} \pm 2e^{-\Gamma t} \sin(\Delta m_s t) \sin \phi_s \right]$	$\sin^2 \psi_T (1 - \sin^2 \theta_T \sin^2 \phi_T)$
3	$\frac{3}{2} A_{\perp}(0) ^2 \left[(1 - \cos \phi_s) e^{-\Gamma_1 t} + (1 + \cos \phi_s) e^{-\Gamma_2 t} \mp 2e^{-\Gamma t} \sin(\Delta m_s t) \sin \phi_s \right]$	$\sin^2 \psi_T \sin^2 \theta_T$
4	$\frac{3}{2} A_0(0) A_{ }(0) \cos \delta_{ } \left[(1 + \cos \phi_s) e^{-\Gamma_1 t} + (1 - \cos \phi_s) e^{-\Gamma_2 t} \pm 2e^{-\Gamma t} \sin(\Delta m_s t) \sin \phi_s \right]$	$\frac{1}{\sqrt{2}} \sin 2\psi_T \sin^2 \theta_T \sin 2\phi_T$
5	$ A_{\perp}(0) A_{\perp}(0) \left[\frac{1}{2} (e^{-\Gamma_1 t} - e^{-\Gamma_2 t}) \cos(\delta_{\perp} - \delta_{ }) \sin \phi_s \pm e^{-\Gamma t} (\sin(\delta_{\perp} - \delta_{ }) \cos \phi_s) \right]$	$-\sin^2 \psi_T \sin 2\theta_T \sin \phi_T$
6	$ A_0(0) A_{\perp}(0) \left[\frac{1}{2} (e^{-\Gamma_1 t} - e^{-\Gamma_2 t}) \cos \delta_{\perp} \sin \phi_s \pm e^{-\Gamma t} (\sin \delta_{\perp} \cos(\Delta \phi_s t) - \cos \delta_{\perp} \sin 2\psi_T \sin 2\theta_T \cos \phi_T) \right]$	$-\frac{1}{\sqrt{2}} \sin 2\psi_T \sin 2\theta_T \cos \phi_T$



CPV in $B_s^0 \rightarrow J/\psi\phi$: OS Tagging

Eur. Phys. J. C 81 (2021) 342

- Knowledge of the initial flavour can improve any CP -violation measurement.
- **Muon/electron tagging**: semi-leptonic decay of B ($b \rightarrow \mu/e$ transition); momentum weighed charge of lepton and tracks in the cone $\Delta R < 0.5$ around the leading lepton $Q_\ell = \frac{\sum_i^{N_{\text{tracks}}} q_i p_{Ti}^{\kappa}}{\sum_i^{N_{\text{tracks}}} p_{Ti}^{\kappa}}$ (constant $\kappa = 1.1$).
- **b -jet-charge tagging**: used if the additional muon/electron is absent; momentum-weighted track-charge in jet.
- Self-tagging $B^\pm \rightarrow J/\psi K^\pm$ channel used for calibration and performance estimation.



Tag method	Efficiency [%]	Effective Dilution [%]	Tagging Power [%]
Tight muon	4.50 ± 0.01	43.8 ± 0.2	0.862 ± 0.009
Electron	1.57 ± 0.01	41.8 ± 0.2	0.274 ± 0.004
Low- p_T muon	3.12 ± 0.01	29.9 ± 0.2	0.278 ± 0.006
Jet	12.04 ± 0.02	16.6 ± 0.1	0.334 ± 0.006
Total	21.23 ± 0.03	28.7 ± 0.1	1.75 ± 0.01



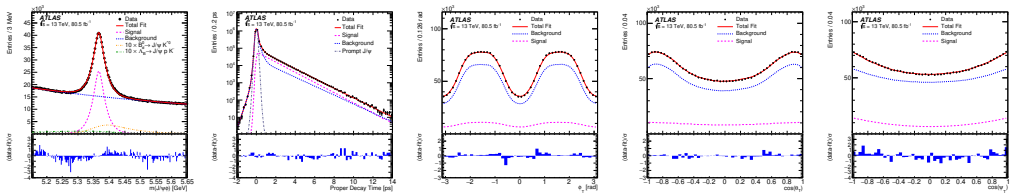
CPV in $B_s^0 \rightarrow J/\psi\phi$: UML Fit

Eur. Phys. J. C 81 (2021) 342

- Unbinned maximum likelihood (UML) fit performed to extract parameters of interest.
- Decay observables: mass, time, angles. Conditional observables: per-candidate tagging and mass/time resolutions ($p_T(B)$ dependent).

$$\ln \mathcal{L} = \sum_{i=1}^N \left\{ w_i \cdot \ln \left(f_{\text{sig}} \cdot \mathcal{F}_{\text{sig}} + f_{\text{sig}} \cdot f_{B_d^0} \cdot \mathcal{F}_{B_d^0} + f_{\text{sig}} \cdot f_{\Lambda_b} \cdot \mathcal{F}_{\Lambda_b} + (1 - f_{\text{sig}}(1 + f_{B_d^0} + f_{\Lambda_b})) \cdot \mathcal{F}_{\text{bck}} \right) \right\}.$$

- Fixed parameters: $\Delta m_s = \text{PDG}$, no direct CP -violation assumed.
- Trigger causing decay time inefficiency, modelled in MC.
- Ratio plots include both stat. and syst. uncertainties; deviations within $2\sigma \Rightarrow$ total uncertainties cover any discrepancy between data and fit model.

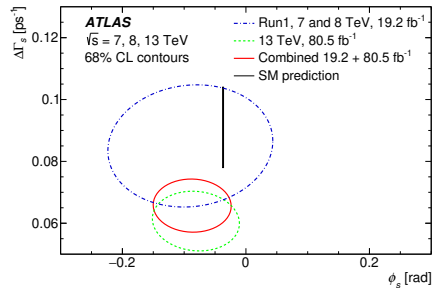


CPV in $B_s^0 \rightarrow J/\psi\phi$: Results

Eur. Phys. J. C 81 (2021) 342

- Likelihood fit determined two solutions for the strong phases, but no effect on the result.

	Value	Stat.	Syst.
ϕ_s [rad]	-0.081	0.041	0.022
$\Delta\Gamma_s$ [ps^{-1}]	0.0607	0.0047	0.0043
Γ_s [ps^{-1}]	0.6687	0.0015	0.0022
$ A_{\parallel}(0) ^2$	0.2213	0.0019	0.0023
$ A_0(0) ^2$	0.5131	0.0013	0.0038
$ A_S(0) ^2$	0.0321	0.0033	0.0046
$\delta_{\perp} - \delta_S$ [rad]	-0.25	0.05	0.04
δ_{\perp} [rad]	3.12 (2.91)	0.11	0.06
δ_{\parallel} [rad]	3.35 (2.94)	0.05	0.09



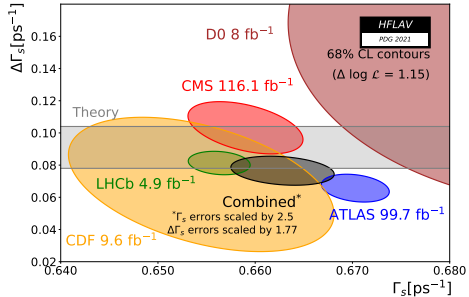
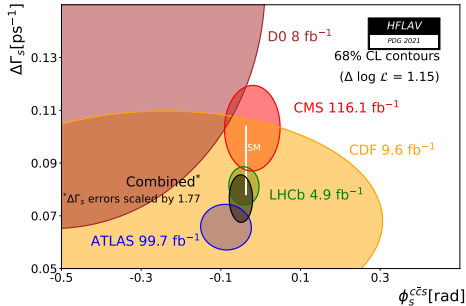
- Weak phase ϕ_s as well as decay width difference $\Delta\Gamma_s$ compatible with SM.
- Dominant systematics on ϕ_s measurement from tagging.
- Statistical (BLUE) combination with Run 1 result.



CPV in $B_s^0 \rightarrow J/\psi\phi$: Comparison

Eur. Phys. J. C 81 (2021) 342

- ATLAS: Still 60 fb^{-1} of 2018 data to be added.
- HFLAV average for PDG 2021: $\phi_s = -0.050 \pm 0.019 \text{ rad}$.



Study of the rare decays of B_s^0 and B^0 mesons
into muon pairs using data collected during
2015 and 2016 with the ATLAS detector



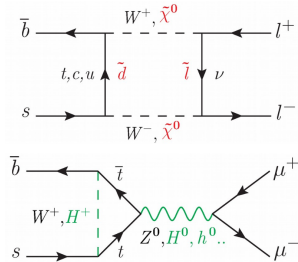
$B_{(s)}^0 \rightarrow \mu\mu$: Introduction

JHEP 04 (2019) 098

- Flavour-changing neutral-current processes highly suppressed in the SM, $B_{(s)}^0 \rightarrow \mu^+\mu^-$ also helicity suppressed $\rightarrow \mathcal{B} \sim 10^{-9}$.
- NP can significantly contribute, modifying the branching ratio.
- 36.2 fb⁻¹ dataset of 2015-2016 data taking, but effectively 26.3 fb⁻¹ for $B_{(s)}^0 \rightarrow \mu\mu$.
- $L_{xy} > 0$ and $m \in (4.0, 8.5)$ GeV requested at HLT.
- $\mathcal{B}(B_{(s)}^0 \rightarrow \mu^+\mu^-)$ measurement relative to $\mathcal{B}(B^\pm \rightarrow J/\psi K^\pm)$; $f_{u,d,s}$ are hadronisation probabilities of a b -quark:

$$\mathcal{B}(B_{(s)}^0 \rightarrow \mu^+\mu^-) = N_{d(s)} \cdot \frac{\mathcal{B}(B^\pm \rightarrow J/\psi K^\pm) \cdot \mathcal{B}(J/\psi \rightarrow \mu^+\mu^-)}{N_{J/\psi K^\pm} \cdot \frac{\epsilon_{\mu^+\mu^-}}{\epsilon_{J/\psi K^\pm}}} \cdot \frac{f_u}{f_{d(s)}}$$

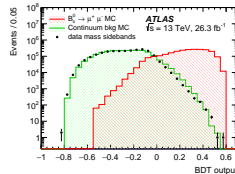
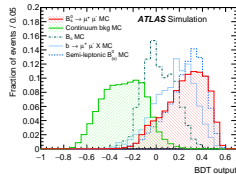
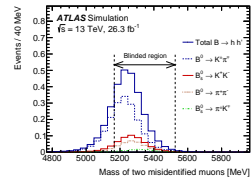
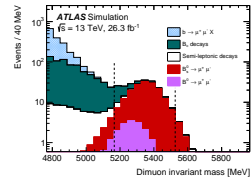
- $B_s^0 \rightarrow J/\psi \phi$ as a control channel.
- Blinded signal di-muon invariant mass region (5166, 5526) MeV.
- BDT based background suppression, trained on sidebands data.
- Yields $N_{d(s)}$ and $N_{J/\psi K^\pm}$ obtained from UML fits to the mass spectra.
- Relative reconstruction efficiencies estimated from corrected MC.



$B^0_{(s)} \rightarrow \mu\mu$: Backgrounds

JHEP 04 (2019) 098

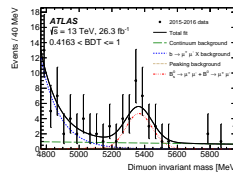
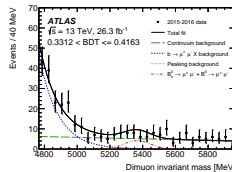
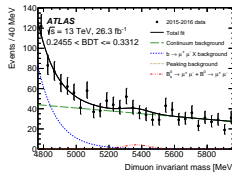
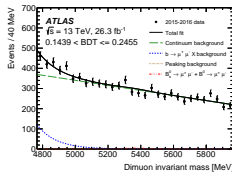
- Partially reconstructed b -hadron decays:
 - Same Vertex: $B^0 \rightarrow \mu\mu X$ decays.
 - Same Side: $b \rightarrow c\mu X \rightarrow s(d)\mu X'$.
 - Semileptonic decay with misidentified hadron.
- Peaking backgrounds:
 - $B^0 \rightarrow h^+ h^-$, both hadrons misidentified as muons.
 - Used tight muon criteria. Only 2.7 ± 1.3 events!
 - Simulated and fixed in the mass fit.
- Continuum background:
 - Combinatorics of muon and uncorrelated hadron decays.
 - Reduced by BDT classifier. Linear shape constrained in the mass fit across BDT bins.



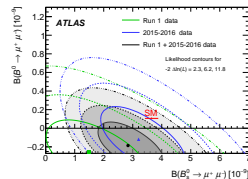
$B_{(s)}^0 \rightarrow \mu\mu$: BDT and signal extraction

JHEP 04 (2019) 098

- Signal region divided into four BDT bins with constant signal efficiency.
- 15 BDT variables (kinematics, isolation, B -vertex separation from PV).
- Validated on $B^\pm \rightarrow J/\psi K^\pm$ and $B_s^0 \rightarrow J/\psi \phi$ channels.
- Simultaneous UML fit to di-muon mass distributions in the four BDT bins to extract $B_{(s)}^0 \rightarrow \mu\mu$ yields.
- Signal model from MC, two double Gaussians, centred on $B_{(s)}^0$ masses.



- **Unconstrained yields:** $N_s = 80 \pm 22$ and $N_d = -12 \pm 20$.
- SM expectation: $N_s = 91$ and $N_d = 10$.
- Run 1 + Run 2 (2015+2016) combined measurement compatible with SM at 2.4σ . Statistic uncertainties dominate.
- Contours obtained using Neyman construction.

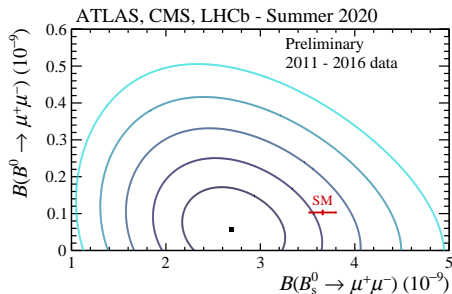
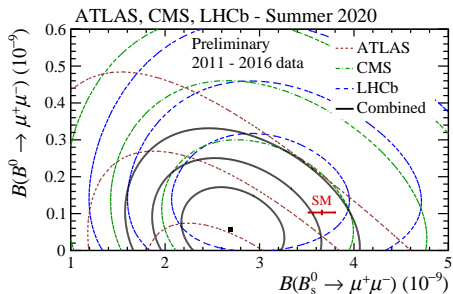


$B_s^0 \rightarrow \mu\mu$: LHC Combination

ATLAS-CONF-2020-049

- ATLAS, CMS and LHCb results.
- Combination from binned 2D profile likelihoods.
- Independent systematics, except for the ratio of fragmentation fractions $\frac{f_d}{f_s}$.

	LHC	SM [2]
$\mathcal{B}(B_s^0 \rightarrow \mu\mu) [10^{-9}]$	$2.69^{+0.37}_{-0.35}$	3.66 ± 0.14
$\mathcal{B}(B^0 \rightarrow \mu\mu) [10^{-10}]$	< 1.9 at 95% CL	1.03 ± 0.05



Summary

- **ATLAS** has produced very **impressive** and **competitive** results in B -physics.
- Working on the updates to the mentioned analyses to full Run 2 statistics, plus:
 - CPV measurement: releasing Δm_s and direct- CP λ , improvements in tagging, fit model, etc.
 - $B_{(s)}^0 \rightarrow \mu\mu$: including $B_s^0 \rightarrow \mu\mu$ lifetime analysis.
- **More public results on ATLAS B-physics TWiki page**
<https://twiki.cern.ch/twiki/bin/view/AtlasPublic/BPhysPublicResults> !

THANK YOU!



BACKUP



CPV in $B_s^0 \rightarrow J/\psi\phi$: Results

Eur. Phys. J. C 81 (2021) 342

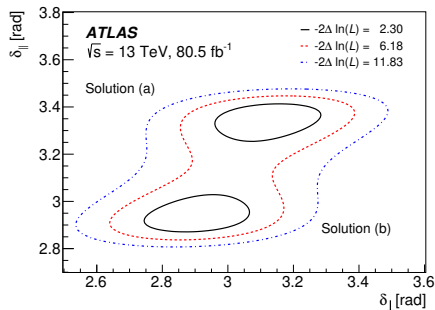
- Likelihood fit determined two solutions for the strong phases δ_{\parallel} and δ_{\perp} .
- Origin – an approximate symmetry in the signal PDF:

$$\{\delta_{\parallel}, \delta_{\perp}, \delta_S\} \rightarrow \{2(\pi - \delta_{\parallel}), \delta_{\perp} + (\pi - \delta_{\parallel}), \delta_{\perp} - \delta_S + (\pi - \delta_{\parallel})\}.$$

This transformation is proportional to $\pi - \delta_{\parallel}$, which from our data is equal to about 0.21.

- $-2\Delta\ln(L)$ between the two solutions is to **0.03**, favouring (a) but without ruling out (b). Only a minor effect on all the variables.

	Value	Stat.	Syst.
ϕ_s [rad]	-0.081	0.041	0.022
$\Delta\Gamma_s$ [ps^{-1}]	0.0607	0.0047	0.0043
Γ_s [ps^{-1}]	0.6687	0.0015	0.0022
$ A_{\parallel}(0) ^2$	0.2213	0.0019	0.0023
$ A_0(0) ^2$	0.5131	0.0013	0.0038
$ A_S(0) ^2$	0.0321	0.0033	0.0046
$\delta_{\perp} - \delta_S$ [rad]	-0.25	0.05	0.04
δ_{\perp} [rad]	3.12	0.11	0.06
	2.91	0.11	0.06
δ_{\parallel} [rad]	3.35	0.05	0.09
	2.94	0.05	0.09



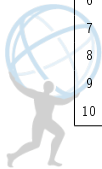
CPV in $B_s^0 \rightarrow J/\psi\phi$: Decay rate

Eur. Phys. J. C 81 (2021) 342

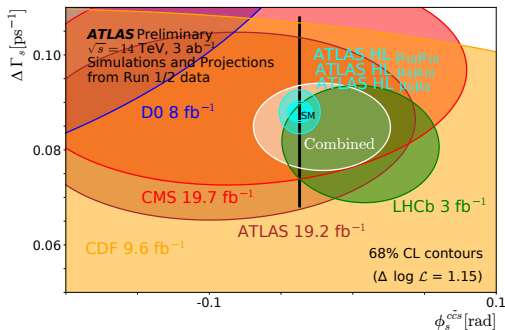
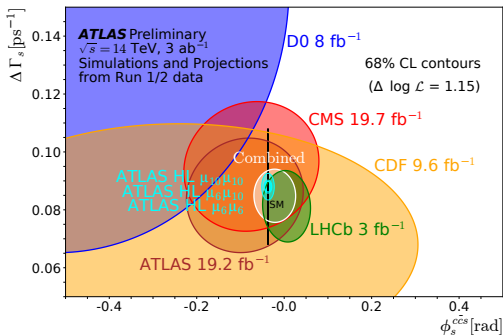
- Ignoring detector effects, the distribution for the time and angles is given by the differential decay rate

$$\frac{d^4\Gamma}{dt d\Omega} = \sum_{k=1}^{10} \mathcal{O}^{(k)}(t) g^{(k)}(\theta_T, \psi_T, \phi_T). \quad (1)$$

k	$\mathcal{O}^{(k)}(t)$	$g^{(k)}(\theta_T, \psi_T, \phi_T)$
1	$\frac{1}{2} A_0(0) ^2 \left[(1 + \cos\phi_s) e^{-\Gamma_{\parallel}^{(+)t}} + (1 - \cos\phi_s) e^{-\Gamma_{\parallel}^{(-)t}} \pm 2e^{-\Gamma_{\parallel}t} \sin(\Delta m_s t) \sin\phi_s \right]$	$2 \cos^2 \psi_T (1 - \sin^2 \theta_T \cos^2 \phi_T)$
2	$\frac{1}{2} A_{\parallel}(0) ^2 \left[(1 + \cos\phi_s) e^{-\Gamma_{\parallel}^{(+)}t} + (1 - \cos\phi_s) e^{-\Gamma_{\parallel}^{(-)t}} \pm 2e^{-\Gamma_{\parallel}t} \sin(\Delta m_s t) \sin\phi_s \right]$	$\sin^2 \psi_T (1 - \sin^2 \theta_T \sin^2 \phi_T)$
3	$\frac{1}{2} A_{\perp}(0) ^2 \left[(1 - \cos\phi_s) e^{-\Gamma_{\perp}^{(+)}t} + (1 + \cos\phi_s) e^{-\Gamma_{\perp}^{(-)t}} \mp 2e^{-\Gamma_{\perp}t} \sin(\Delta m_s t) \sin\phi_s \right]$	$\sin^2 \psi_T \sin^2 \theta_T$
4	$\frac{1}{2} A_0(0) A_{\parallel}(0) \cos\delta_{\parallel} \left[(1 + \cos\phi_s) e^{-\Gamma_{\parallel}^{(+)}t} + (1 - \cos\phi_s) e^{-\Gamma_{\parallel}^{(-)t}} \pm 2e^{-\Gamma_{\parallel}t} \sin(\Delta m_s t) \sin\phi_s \right]$	$\frac{1}{\sqrt{2}} \sin 2\psi_T \sin^2 \theta_T \sin 2\phi_T$
5	$ A_{\parallel}(0) A_{\perp}(0) \left[\frac{1}{2}(e^{-\Gamma_{\parallel}^{(+)}t} - e^{-\Gamma_{\parallel}^{(-)t}}) \cos(\delta_{\perp} - \delta_{\parallel}) \sin\phi_s \pm e^{-\Gamma_{\parallel}t} (\sin(\delta_{\perp} - \delta_{\parallel}) \cos(\Delta m_s t) - \cos(\delta_{\perp} - \delta_{\parallel}) \cos\phi_s \sin(\Delta m_s t)) \right]$	$-\sin^2 \psi_T \sin 2\theta_T \sin \phi_T$
6	$ A_0(0) A_{\perp}(0) \left[\frac{1}{2}(e^{-\Gamma_{\perp}^{(+)}t} - e^{-\Gamma_{\perp}^{(-)t}}) \cos\delta_{\perp} \sin\phi_s \pm e^{-\Gamma_{\perp}t} (\sin\delta_{\perp} \cos(\Delta m_s t) - \cos\delta_{\perp} \cos\phi_s \sin(\Delta m_s t)) \right]$	$\frac{1}{\sqrt{2}} \sin 2\psi_T \sin 2\theta_T \cos \phi_T$
7	$\frac{1}{2} A_S(0) ^2 \left[(1 - \cos\phi_s) e^{-\Gamma_{\parallel}^{(+)}t} + (1 + \cos\phi_s) e^{-\Gamma_{\parallel}^{(-)t}} \mp 2e^{-\Gamma_{\parallel}t} \sin(\Delta m_s t) \sin\phi_s \right]$	$\frac{2}{3} (1 - \sin^2 \theta_T \cos^2 \phi_T)$
8	$\alpha A_S(0) A_{\parallel}(0) \left[\frac{1}{2}(e^{-\Gamma_{\parallel}^{(+)}t} - e^{-\Gamma_{\parallel}^{(-)t}}) \sin(\delta_{\parallel} - \delta_S) \sin\phi_s \pm e^{-\Gamma_{\parallel}t} (\cos(\delta_{\parallel} - \delta_S) \cos(\Delta m_s t) - \sin(\delta_{\parallel} - \delta_S) \cos\phi_s \sin(\Delta m_s t)) \right]$	$\frac{1}{3} \sqrt{6} \sin \psi_T \sin^2 \theta_T \sin 2\phi_T$
9	$\frac{1}{2}\alpha A_S(0) A_{\perp}(0) \sin(\delta_{\perp} - \delta_S) \left[(1 - \cos\phi_s) e^{-\Gamma_{\perp}^{(+)}t} + (1 + \cos\phi_s) e^{-\Gamma_{\perp}^{(-)t}} \mp 2e^{-\Gamma_{\perp}t} \sin(\Delta m_s t) \sin\phi_s \right]$	$\frac{1}{3} \sqrt{6} \sin \psi_T \sin 2\theta_T \cos \phi_T$
10	$\alpha A_0(0) A_S(0) \left[\frac{1}{2}(e^{-\Gamma_{\parallel}^{(+)}t} - e^{-\Gamma_{\parallel}^{(-)t}}) \sin\delta_S \sin\phi_s \pm e^{-\Gamma_{\parallel}t} (\cos\delta_S \cos(\Delta m_s t) + \sin\delta_S \cos\phi_s \sin(\Delta m_s t)) \right]$	$\frac{4}{3} \sqrt{3} \cos \psi_T (1 - \sin^2 \theta_T \cos^2 \phi_T)$



Prospects of CPV Measurements (Upgraded ATLAS, HL-LHC, [3])



REFERENCES



References |

- [1] J. Charles *et al.*, *Current status of the standard model CKM fit and constraints on $\Delta F = 2$ new physics*, Phys. Rev. D 91 (2015) no.7, 073007, numbers updated using the results from the 2019 values in https://ckmfitter.in2p3.fr/www/results/plots_summer19/ckm_res_summer19.html.
- [2] M. Beneke, C. Bobeth and R. Szafron, *Power-enhanced leading-logarithmic QED corrections to $B_q \rightarrow \mu^+ \mu^-$* , JHEP 10 (2019), 232.
- [3] ATLAS and CMS Collaborations, *Report on the Physics at the HL-LHC and Perspectives for the HE-LHC*, arXiv:1902.10229 [hep-ex].

